Journal of Thermal Analysis and Calorimetry, Vol. 75 (2004) 655–660

CRYSTALLIZATION OF $Co_{75-X}Fe_XGe_{15}B_{10}$ AMORPHOUS ALLOYS

M. D. B. Barroso [1], *T. A. A. Melo* [2], *Shiva Prasad* [3], *R. M. Gomes* [2], *I. C. E. S. G. Lima* [2], *A. G. Souza* [4] *and S. J. G. Lima* [2*]

[1]Instituto Centro de Ensino Tecnológico, CENTEC, Universidade Federal da Paraíba, Paraíba, Brazil
[2]Laboratório de Solidificação Rápida, CT-DTM, Universidade Federal da Paraíba, Campus I, Cidade Universitária, 58059-900 João Pessoa, Paraíba, Brazil
[3]Universidade Federal de Campina Grande, Campina Grande, Paraíba, Brazil
[4]Laboratório de Termoquímica e Materiais, CCEN-DQ, Universidade Federal da Paraíba, Campus I, 58059-900, João Pessoa, Paraíba, Brazil

Abstract

The crystallization behavior of $Co_{75-x}Fe_xGe_{15}B_{10}$ (x=3.0, 4.6 and 6.0) amorphous alloys was monitored by differential thermal analysis and thermo-mechanical analysis. The crystallization process of the melt spun ribbons was interrupted at 450, 525, 650, 800 and 900°C and their microstructures were investigated by X-ray diffractometry. It was observed that the crystallization occurs in a sequential mode attributed to the formation of different types of precipitates. It was shown that the crystallization products change as a function of Fe content. After full crystallization, GeFe, Co_3B, $FeGe_2$ and Co_2Ge compounds were found as well as a Co rich solid solution.

Keywords: amorphous alloys, crystallization, thermal analysis

Introduction

Metallic glasses suffer from thermal instability which impedes their applications at higher temperatures. In such case, the study of the crystallization behavior is of great importance due to their structural evolution and the formation of new nanoscale precipitates [1]. Researches on the crystallization of amorphous alloys are impulsioned by the promising new properties [2]. Currently, several studies have been carried out on (Co, Fe, Ni) – (Si, B, C) amorphous alloys system [3–7] and many of them were particularly addressed to the microstructural investigations of the CoFeSiB amorphous alloys. Since Ge and Si elements are thought to display similar features the substitution of Si by Ge in the FeSiB alloys may also lead to the achievement of amorphous structure [8]. However, studies on the CoFeGeB alloy systems are still scarce. Then, the influence of Ge on the crystallization behavior is not fully investigated yet. In the present work cobalt based amorphous ribbons with Ge addition were produced by

* Author for correspondence: E-mail: jackson@lsr.ct.ufpb.br

1388–6150/2004/ $ 20.00

Akadémiai Kiadó, Budapest
Kluwer Academic Publishers, Dordrecht

melt-spinning process. The crystallization behavior of these alloys was investigated by means of differential thermal analysis (DTA) thermo-mechanical analysis (TMA), and X-ray diffraction (XRD) techniques.

Experimental

The $Co_{72}Fe_3Ge_{15}B_{10}$, $Co_{70.4}Fe_{4.6}Ge_{15}B_{10}$ and $Co_{69}Fe_6Ge_{15}B_{10}$ amorphous alloys were produced by melt-spinning technique [9, 10]. Ribbons with, approximately, 30 μm thickness and 2.0 mm width were obtained under argon atmosphere, with a copper wheel at 2000 rpm and ejection pressure of 0.2 bar. The crystallization behavior was investigated by means of DTA and TMA up to of 700°C at a heating rate of 10 K min^{-1}. Initially, in order to guide the selection of thermal heat treatments condition DSC scan was performed. To investigate the structural evolution thermal heat treatments were carried out at 450, 525 and 650°C followed by water quenching. For comparison, a complete crystallization was also done at 800 and 900°C for 1.0 and 2.0 h followed by furnace cooling. The heat treated ribbons structures were investigated by XRD using the CuK_α radiation=0.15406 nm.

Results and discussion

The DTA and TMA curves are shown in Figs 1 and 2, respectively. Several exothermic reactions can be observed indicating that crystallization phenomena occur at least in two steps. The onset temperatures of crystallization were determined from DTA and TMA curves. However, only the onset temperature of the first step was accurately determined because the superposition of the subsequent reactions did not allow to measure the onset temperatures of each reaction.

The alloy containing 3.0% Fe displays a first crystallization step which was not detected in other alloys. In the alloy containing 4.6% Fe this first step of crystallization superpose with the second subsequent reaction. The onset temperatures

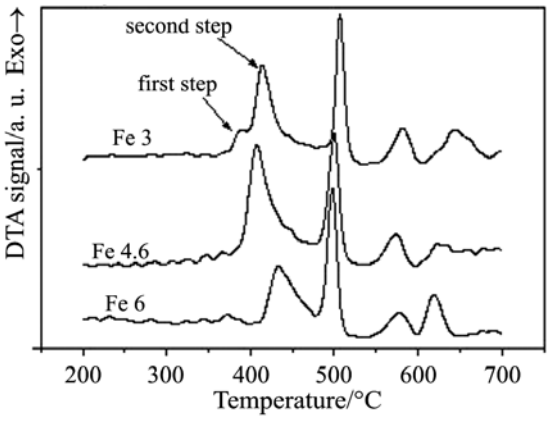

Fig. 1 DTA curves of CoFeGeB ribbons alloys

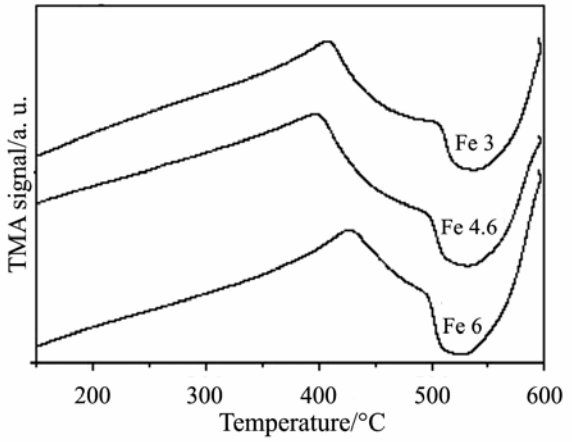

Fig. 2 TMA curves of CoFeGeB ribbons alloys

were 385, 392 and 411°C for alloys containing 3.0% Fe, 4.6% Fe and 6.0% Fe, respectively. Also, as the Fe content increases to 6.0% the onset temperature of the second crystallization reaction shifts to higher temperatures. The XRD patterns of the heat treated ribbons, with 3.0, 4.6 and 6.0% Fe, at different temperatures, are shown in Figs 3–5, respectively. The detected phases are marked on the X-ray diffractograms.

For all alloys ribbons heat treated at 450°C, the existence of sharp and very broad peaks was detected indicating that the microstructure consists of a mixture of amorphous and crystalline phases. These sharp peaks are more evidenced in the alloy with 4.6% Fe and was indexed as being the CoFe intermetallic compound (Pm3m, a=0.2857 nm), which is in accordance with [11]. Additionally, it is interesting to note that, in alloys containing 3.0% Fe the hexagonal Co solid solution ($Co_{(s)}$-h) commences to appear which was detected in the alloys containing 4.6 and 6.0% Fe. This result suggests that the first

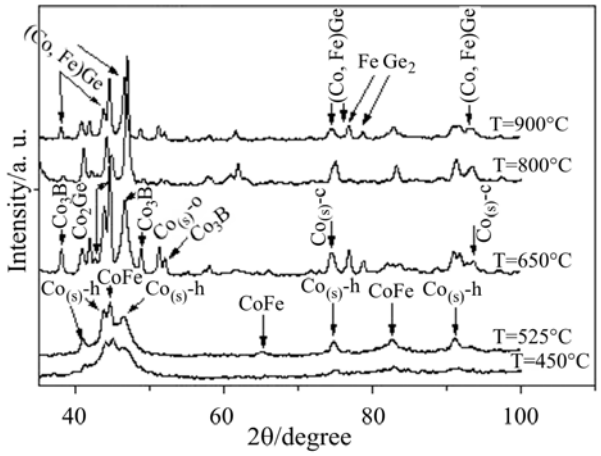

Fig. 3 X-ray diffractograms of heat treated $Co_{72}Fe_3Ge_{15}B_{10}$ alloy at different temperatures

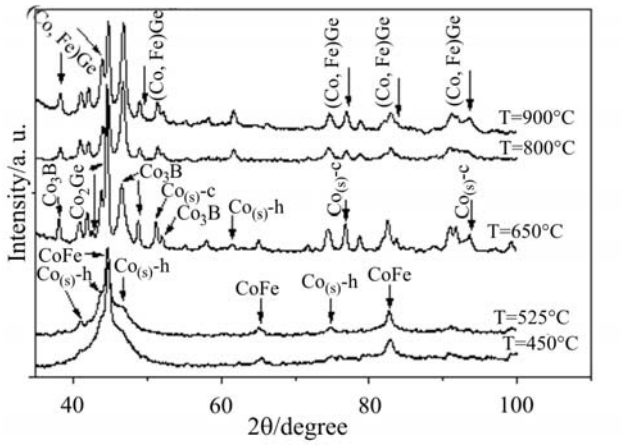

Fig. 4 X-ray diffractograms of heat treated $Co_{70.4}Fe_{4.6}Ge_{15}B_{10}$ alloy at different temperatures

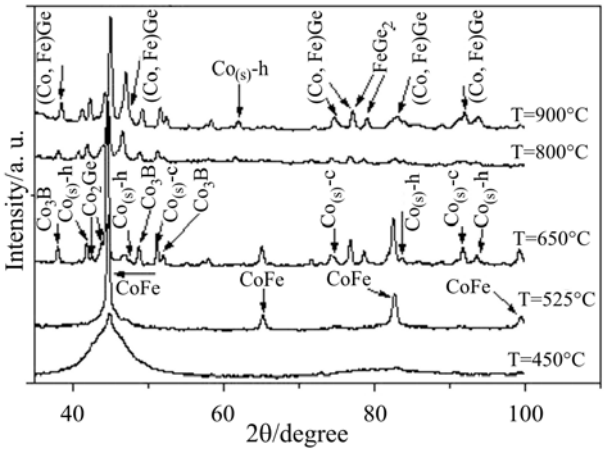

Fig. 5 X-ray diffractograms of heat treated $Co_{69}Fe_6Ge_{15}B_{10}$ alloy at different temperatures

step observed on the DTA curves of the alloy containing 3.0% Fe is attributed to the beginning of the crystallization of the $Co_{(s)}$-h. Further increases in the heat treatment temperature to 525°C the peaks corresponding to the CoFe intermetallic compound becomes sharper and remains stable up to ~650°C. Additionally, at 525°C the $Co_{(s)}$-h solid solution ($P6_3/mmc$, a=0.251 nm, c=0.418 nm) was also clearly observed in the alloys containing 4.6% Fe. On the other hand, in the alloys containing 6.0% Fe this phase was not detected indicating that an increase in Fe content seems to inhibit the formation of the Co rich solid solution. It is also interesting to point out that, the Co_3B compound can also be detected in all alloys after heat treated at 650°C.

The XRD patterns of the alloys heat treated at 650°C revealed the following phases: $Co_{(s)}$-h with lattice parameters a=0.254 nm and c=0.411 nm; cubic Co solid solution with a=0.356 nm, Co_2Ge, Co_3B, CoFe and $FeGe_2$. In the alloys heat treated at 800°C the cubic Co solid solution phase and the CoFe compound were no longer de-

tected, giving way to the formation of an isomorphous CoGe phase ($P2_13$), the lattice parameter of which decreases with increasing the Fe content up to 4.6% Fe where an abrupt drop is observed in the lattice parameter and an increase again for alloys containing 6.0% Fe, as shown in Table 1. Further experiments are still necessary to provide a satisfactory explanation of this lattice parameter drop for alloys containing 4.6% Fe.

Table 1 Lattice parameter change of the (Co, Fe)Ge phase as a function of the Fe content for alloys heat treated at 800°C

Lattice parameter	Fe content/%			
	0.0	3.0	4.6	6.0
a/nm	0.4637	0.4633	0.4611	0.4632

Thus, it is plausible to assume that the Co solid solution, which was detected in the alloys heat treated at 650°C is in fact Co–Ge solid(s) solution(s). On the other hand, according to the binary Co–Ge equilibrium diagram the solid solubility of Ge in the Co phase between 700 and 800°C is ~12 mass%, being that a higher solubility can be reached by rapid solidification. When heat treated at 800°C and slowly cooled to room temperature the Co–Ge solid solution releases the Ge atoms to form the (Co, Fe)Ge compound. It is also important to notice that at room temperature the solid solubility of Ge in Co is negligibly small. The other phases (Co_3B, $FeGe_2$ and Co_2Ge) remain unchanged. In heat treated alloys at 900°C, no new microstructural changes were observed.

Conclusions

DTA, TMA and XRD techniques were used to investigate the crystallization behavior of $Co_{75-x}Fe_xGe_{15}B_{10}$ (x=3.0, 4.6 and 6.0) alloys. The conclusions can be summarized as follows:

i) It was observed by DTA and TMA analysis, that the crystallization of the alloys strongly depends on the Fe content and takes place in more than two stages. Also, the onset temperature of crystallization increases with increasing the Fe content;

ii) The first step of crystallization of the alloys with 4.6% Fe and 6.0% Fe was attributed to the precipitation of the CoFe(cubic) phase. In the alloys containing 3.0% Fe the first exothermic reaction observed on the DTA curves was due to the formation of hexagonal Co solid solution. Besides, the formation of the hexagonal Co solid solution is retarded with increasing of the Fe content;

iii) In the alloys heat treated at 650°C, the following phases were identified: Co(hex.) solid solution, Co(cubic) solid solution, Co_2Ge, Co_3B, CoFe and $FeGe_2$;

iv) After heat treatment at 800°C followed by slow cooling to room temperature the Co(cubic) phase and CoFe compound were no longer detected. On the other hand, the formation of the (Co, Fe)Ge compound was observed which is an isomorphous of the CoGe phase.

The authors are grateful to the Brazilian PADCT/CNPq and CAPES for supporting this work.

References

1 J. M. Dubois and G. Le Caer, Acta Metall., (1984) 2101.
2 K. Chrissafis, J. Therm. Anal. Cal., 73 (2003) 745.
3 N. Imamura and T. Kobayashi, IEEE Trans. Magn., 12 (1976) 779.
4 M. N. Baibich, J. M. Broto, A. Fert, F. N. Van Dau and F. Petroff, Phys. Rev. Letter, 61 (1988) 2472.
5 F. L. Barquín, J. R. Fernández and J. C. Gómez-Sal, J. Magn. Magn. Mater., 83 (1990) 357.
6 A. D. Santos, A. S. Medici and F. P. Missell, J. Magn. Magn. Mater., 60 (1986) 153.
7 S. Al Bijat, R. Iraldi, C. Cunat, G. Le Caer, J. M. Dubois and C. Tete, Proc. of the 4th Int. Conf. on Rapidly Quenched Metals, Sendai-Japan 1981.
8 J. R. Bedell, U. S. Patent Nº 3 862 658, Jan. 28, 1975.
9 C. K. N. Oliveira, MS Dissertation, CPGEM/CT/UFPB, João Pessoa, PB, Brasil 1996.
10 J. J. Suñol, M. T. Clavaguera-Mora and N. Clavaguera, J. Therm. Anal. Cal., 72 (2003) 347.
11 V. Pearson's and L. D. Calvert, Pearson's Handbook of Crystallographic Data for Intermetallic Phases, ASM, 2 (1985) 1750.